Mathematical Analysis & Convex Optimization

Vol. 4 (2023), No. 2, 81–90
https:\\ maco.lu.ac.ir
DOI: 10.22034/maco.4.2.8

Research Paper

A WATERMARKING TECHNIQUE USING FINITE RIDGELET TRANSFORM AND BIDIAGONAL SVD

FARZANEH SALARI

Abstract. The ease with which digital images can be manipulated with readily available editing tools highlights the critical need for robust copyright protection mechanisms. Digital watermarking tackles this challenge by embedding imperceptible ownership information within images. However, striking a balance between transparency (invisibility of the watermark) and robustness against attacks remains a significant hurdle. This paper proposes a watermarking method that uses the combined strengths of Finite Ridgelet Transform (FRIT) and Bidiagonal Singular Value Decomposition (BSVD). Our approach first pre-processes the image using FRIT to extract prominent features. Subsequently, the watermark is imperceptibly embedded into the singular values obtained from the FRIT coefficients. Our evaluation using standard sample images confirms high visual quality and robustness to attacks for the proposed method.

MSC(2010): 42C40; 42C15; 68U10; 94A08.
Keywords: digital watermarking, finite ridgelet transform, bidiagonal singular value decomposition.

1. Introduction and Background

Digital watermarking has emerged as a prominent technique for safeguarding ownership and copyright protection of multimedia content. The core principle lies in embedding a subtle and imperceptible mark, such as a logo or signature, within the host image. This mark serves as a unique identifier, establishing ownership and facilitating content authentication. However, achieving a balance between robustness (resistance to attacks) and imperceptibility (invisibility to the human eye) presents a significant challenge [5].

Watermarking techniques can be broadly classified into two categories: blind and non-blind. Blind watermarking allows for watermark retrieval without the original unwatermarked image, while non-blind methods necessitate it. Furthermore, these techniques can be categorized based on the domain of watermark embedding: spatial or frequency [10, 14]. Spatial domain methods embed the watermark directly into the pixel values of the image. While computationally efficient, they are often susceptible to attacks that alter the image content. Conversely, frequency domain methods embed the watermark into the transformed frequency coefficients of the image, typically obtained using Discrete Fourier Transform (DFT) [11], Discrete Cosine Transform (DCT)[9] or Discrete Wavelet Transform (DWT)[1]. These methods offer enhanced robustness due to the inherent characteristics of the frequency domain.

Date: Received: May 5, 2023 , Accepted: December 26, 2023.

Among various frequency transforms, DWT has gained significant traction in watermarking due to its alignment with the human visual system (HVS). This alignment allows for watermark embedding in regions less perceptible to the human eye, thereby enhancing transparency. However, limitations associated with directionality and high-dimensional singularity representation in DWT have spurred advancements like wavelet packets, multi-wavelet transforms, and multi-directional wavelets (e.g., curvelets and ridgelets) [12, 14].

Ridgelets, introduced to address limitations of wavelets in representing line singularities in higher dimensions [3], offer a powerful tool for image watermarking. The finite ridgelet transform (FRIT) facilitates the implementation of ridgelets in a discrete manner, specifically designed for representing linear singularities [4]. FRIT essentially transforms line singularities into point singularities using the Radon transform, enabling efficient processing using one dimensional wavelet transform.

Matrix factorization, a cornerstone technique in linear algebra, plays a vital role in various applications, including watermarking. Singular Value Decomposition (SVD) is a widely employed factorization method in watermarking [8]. Bidiagonal SVD (BSVD) can be viewed as an extension of SVD, offering an alternative and potentially more efficient approach for matrix decomposition. Notably, while the singular values obtained from both SVD and BSVD are identical, BSVD offers advantages in terms of computational efficiency [2, 7].

This paper introduces a new method for watermarking digital images. This technique combines the advantages of two existing methods: FRIT and BSVD. The proposed method works in several steps. First, it applies FRIT to the image being watermarked. FRIT transforms the image into a new representation that highlights specific features, like lines and edges. This transformed image is then broken down further using BSVD. BSVD decomposes the image into its basic building blocks, allowing for manipulation of specific components. In our approach, the watermark information, which is usually another image, directly alters the singular values obtained from the FRIT coefficients. These singular values represent the most important information in the transformed image. By carefully modifying them, we can embed the watermark into the host image without significantly changing its appearance.

The remaining sections of this paper are organized as follows: Section 2 provides a basic explanation of the underlying principles behind FRIT and BSVD. Section 3 describes the FRIT-BSVD watermarking method in depth. Section 4 details the experiments and their outcomes, followed by a concluding summary of key findings.

2. **Foundational Concepts**

This section explores two image processing techniques: FRIT, excelling at analyzing images with straight edges through its frequency domain decomposition, and BSVD, a variant of SVD that achieves decomposition in fewer steps. Both techniques play significant roles in various image processing applications.

2.1. **Finite Ridgelet Transform (FRIT).**

FRIT has gained prominence as a method for spectral decomposition of digital images. It achieves this by analyzing the image in the frequency domain along linear features. This analysis is accomplished through the Finite Radon Transform (FRAT), which calculates the discrete summation of pixel intensities along specific line segments. These line segments, analogous to those used in the continuous Radon transform, are adapted to the finite grid structure of digital images. This adaptation allows FRIT to effectively capture the spectral characteristics of structures with straight edges, making it particularly valuable for various image processing applications.

FRIT employs a two-step process for image representation. In the first step, FRAT decomposes the image into components aligned with linear features. The second step utilizes a one-dimensional wavelet transform for further analysis. FRAT operates within a finite field denoted by $Z_p = \{1, 2, 3, \ldots, p-1\}$, where p is a prime number and calculations exhibit periodic wrapping around p. This finite field is crucial for adapting the continuous Radon transform to the discrete structure of digital images. Within this framework, the FRAT analyzes real-valued functions defined on a two-dimensional grid constructed from elements of Z_p. The specific transformation for a function f can be expressed mathematically as:

$$r_k[l] = FRAT_f(k,l) = \frac{1}{\sqrt{(p)}} \sum_{(i,j)\in L_{k,l}} f[i,j] \tag{2.1}$$

where $L_{k,l}$ denotes the set of points that define a straight line segment on the Z_p^2 as follows:

$$\begin{aligned} L_{k,l} &= \{(i,j) : j = ki + l \ (mod\ p), i \in Z_p\}, 0 \le k < p, \\ L_{p,l} &= \{(l,j) : j \in Z_p\}. \end{aligned} \tag{2.2}$$

Benefiting from the invertibility of FRAT, FRIT itself can also be inverted. This desirable property is achieved by applying a one-dimensional wavelet transform to each sequence of projections $r_k[0], r_k[1], \ldots, r_k[p-1]$ obtained from the directional FRAT decomposition.

2.2. **Bidiagonal Singular value decomposition (BSVD).** Singular Value Decomposition (SVD) is a well-established tool in numerical analysis for matrix decomposition. This decomposition finds significant applications in image processing tasks such as compression and watermarking. SVD can be used independently or integrated with other image processing techniques for watermarking [13, 15]. SVD possesses two key characteristics that make it well-suited for watermarking applications:

(1) Resilience to Noise: Minor image distortions have minimal impact on singular values, ensuring robustness.
(2) Capturing Image Information: By capturing an image's core algebraic properties, singular values offer a robust foundation for watermark embedding.

SVD decomposes an $m \times n$ matrix I into three separate matrices: $I = U \times S \times V^T$, where U and V are orthogonal matrices and S is a diagonal matrix containing the singular values (λ_i) arranged in descending order $(i = 1, \ldots, m)$.

Building upon SVD, Bidiagonal SVD (BSVD) offers an alternative approach to spectral decomposition. Notably, both techniques produce similar singular values, but their computational methods for calculating these values differ [2]. BSVD computation involves two key steps:

Step1 (Bidiagonalization): This step transforms the input matrix I $(m \times n)$ into a simpler form called a bidiagonal matrix. Equation (2.3) shows this transformation:

$$I = U_I \times P \times V_I^T \tag{2.3}$$

Here, U_I is an $m \times n$ orthonormal matrix, V_I is an $n \times n$ unitary matrix, and P is a special $n \times n$ matrix with non-zero entries only on the main diagonal and the superdiagonal (strictly upper bidiagonal).

Bidiagonalization shares similarities with SVD decomposition. However, it achieves the decomposition in a finite number of operations, while SVD uses iterative methods to find singular values. Common methods for bidiagonalization include:

- Golub-Kahan Bidiagonalization: This approach employs Householder reflections applied sequentially from left and right sides of the matrix for dense matrices.
- Golub-Kahan-Lanczos Method: For large matrices, an iterative approach using the Lanczos method is used.

Step 2 (SVD of the Bidiagonal Matrix): The second step applies SVD to the bidiagonal matrix P obtained in step 1. This is shown in Equation (2.4):

$$P = U_P \times S \times V_P^T \tag{2.4}$$

Here, U_P and V_P are both unitary matrices, and S is a diagonal matrix defined as:

$$S = diag(\lambda_1, \lambda_2, \ldots, \lambda_r) \tag{2.5}$$

The diagonal elements of $S(\lambda_i)$ represent the singular values of matrix P, with r being the minimum of m and n. These singular values are arranged in descending order ($\lambda_1 \geq \lambda_2 \geq ... \geq \lambda_r$).

Combining the Steps (The BSVD Decomposition): By substituting Equation (2.4) into Equation (2.3), we obtain the complete BSVD decomposition of matrix I:

$$I = U_I \times U_P \times S \times V_P^T \times V_I^T \tag{2.6}$$

This final equation shows how I is decomposed into a product of five matrices, revealing the underlying structure of BSVD.

SVD and BSVD tackle data analysis differently. Research [2] compared their effectiveness in reconstructing images using their inverse forms. The study revealed that BSVD achieved superior results, especially for datasets containing non-integer numbers, as measured by PSNR.

3. The Proposed Method

This paper presents a watermarking method using FRIT and BSVD. FRIT extracts image features, and BSVD captures their spectral essence. The watermark is then embedded into these singular values. Retrieval utilizes a similar process in reverse to extract the watermark.

3.1. The watermark embedding process.

Step 1: Apply FRIT to the original image (I). This step extracts features aligned with linear structures in the image, resulting in a matrix of ridgelet coefficients (R).

$$R = FRIT(I) \tag{3.1}$$

Step 2: Perform BSVD on the ridgelet coefficient matrix (R). This step decomposes R into its singular values, which capture the essential spectral information of the image.

$$[U_I, U_P, S, V_I, V_P] = BSVD(R) \tag{3.2}$$

Step 3: Embed the watermark image (W) into the singular values (S) using a scaling factor (α). This modifies the singular values to imperceptibly encode the watermark.

$$W' = S + \alpha.W \tag{3.3}$$

Step 4: Reconstruct a modified singular value matrix (S') by Appling SVD on the modified watermark (W').

$$\left[U, S', V\right] = SVD(W') \tag{3.4}$$

Step 5: Apply the inverse BSVD operation to reconstruct a modified version of the ridgelet coefficient matrix (R').

$$R' = U_I \times U_P \times S' \times V_P^T \times V_I^T \tag{3.5}$$

Step 6: Perform the inverse FRIT operation on the modified ridgelet coefficients (R'). This step transforms the coefficients back into the spatial domain, resulting in the watermarked image (I^*).

3.2. **The watermark extraction process.** The watermark is retrieved using a procedure that reverses most steps from the embedding process.

Step 1: Similar to embedding, apply FRIT to the watermarked image (I^*), resulting in a matrix of ridgelet coefficients (R^*).

$$R^* = FRIT(I^*) \tag{3.6}$$

Step 2: Perform BSVD on the extracted ridgelet coefficient matrix (R^*). This step decomposes R^* into its singular values, containing the embedded watermark information.

$$[U_{I^*}, U_{P^*}, S^*, V_{I^*}, V_{P^*}] = BSVD(R^*) \tag{3.7}$$

Step 3: Utilize the original embedding information (U and V matrices) obtained during the embedding process. Combine these with the modified singular values (S^*) from step 2 by an inverse SVD to estimate the modified watermarked (W').

$$W' = U \times S^* \times V \tag{3.8}$$

Step 4: Reconstruct the extracted watermark image (W^*) using the matrix W' obtained in step 3. This involves reversing the modifications made during embedding process.

$$W = \frac{W' - S}{\alpha} \tag{3.9}$$

4. Experimental results and comparative analysis

The performance of the proposed FRIT-BSVD watermarking method was evaluated using a comprehensive set of experiments.

4.1. **Dataset.**

- Host Images: A diverse set of five grayscale images (257 x 257 pixels each) was selected from the USC-SIPI image database to ensure the generalizability of the method (Figure 1).
- Watermark: A separate grayscale watermark image of the same size was used for all experiments (Figure 1).

The watermarking process incorporated a pre-defined scaling factor ($\alpha = 0.01$) in both embedding and extraction stages to achieve an optimal trade-off between imperceptibility and robustness.

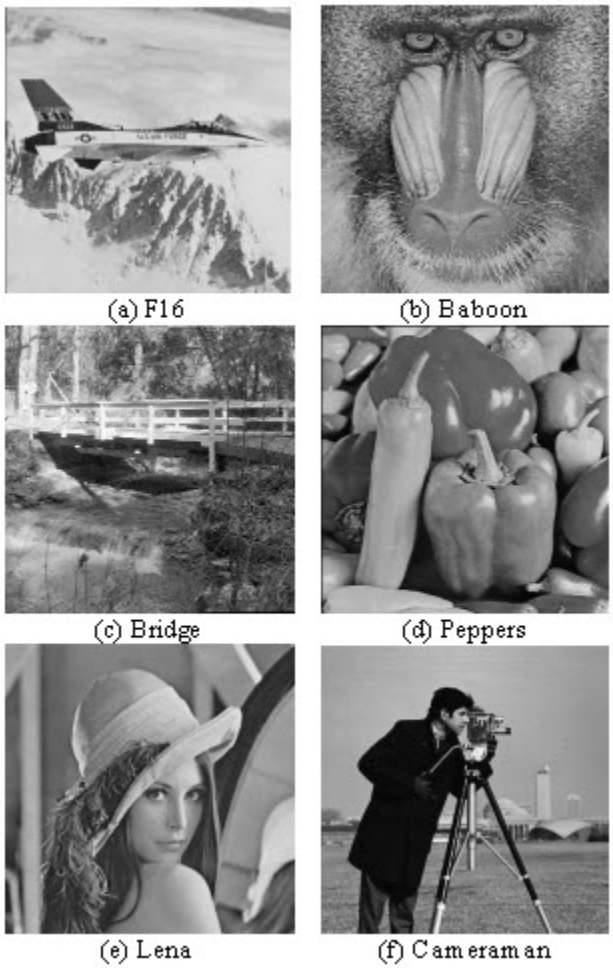

FIGURE 1. (a) to (e): The host images and (f): The watermark image

4.2. **Evaluation Metrics.** The efficacy of watermarking schemes are assessed using two key metrics: transparency and robustness.

Transparency measures the imperceptibility of the watermark. It is evaluated using two well-established metrics:

- Peak Signal-to-Noise Ratio (PSNR): PSNR quantifies the maximum possible signal power (peak signal) compared to the power of corrupting noise (background noise). Higher PSNR values indicate better visual quality. The mathematical formula for PSNR is provided below:

$$PSNR = 10 \log_{10} \left(\frac{MAX(p)^2}{MSE} \right), \tag{4.1}$$

Within the formula, $MAX(p)$ denotes the maximum intensity a single pixel can hold in the image. The Mean Squared Error (MSE) metric, on the other hand, quantifies the average squared difference in intensity values between the original and watermarked

versions. The calculation for MSE is presented below:

$$MSE = \frac{1}{xy}\sum_{p=0}^{x-1}\sum_{q=0}^{y-1}[O(p,q) - W(p,q)]^2, \tag{4.2}$$

The equation uses x and y to stand for the image's width and height. Additionally, it uses $O(p,q)$ and $W(p,q)$ to represent the color value of the original image and the watermarked image at specific points (p,q) on the grid, respectively.

- Structural Similarity Index Measure (SSIM): SSIM stands out from traditional metrics like PSNR by prioritizing the preservation of structural details within images. It accomplishes this through a window-based analysis, where the image is subdivided into smaller regions for evaluation. The specific calculation for SSIM is presented in the following equation:

$$SSIM(O,W) = \frac{(2M_oM_w + c_1)(2V_{ow} + c_2)}{(M_o^2 + M_w^2 + c_1)(V_o^2 + V_w^2 + c_2)} \tag{4.3}$$

where, M_o and M_w represent the average values of the original image (O) and the watermarked image (W), respectively. Similarly, V_o^2 and V_w^2 capture the variations (variances) within O and W. The term V_{ow} reflects the co-variation between O and W, indicating how their intensity values change together. Finally, the constants c_1 and c_2 are included to prevent calculation issues when dealing with very small values, which can happen during mathematical operations.

Robustness, a crucial requirement for watermarks, is resilience against attacks. Robustness is assessed using the Normalized Cross Correlation (NC) metric, which serves as a quantitative measure of similarity between the original watermark (W) and the watermark extracted (W') following an attack. It essentially captures how well the retrieved watermark aligns with the original after undergoing potential distortions. The calculation for NC is presented in the equation below:

$$NC(W,W') = \frac{\sum_{p=0}^{x-1}\sum_{q=0}^{y-1}(W(p,q) - M_w)(W'(p,q) - M_{w'})}{\sqrt{\sum_{p=0}^{x-1}\sum_{q=0}^{y-1}(W(p,q) - M_w)^2}\sqrt{\sum_{p=0}^{x-1}\sum_{q=0}^{y-1}(W'(p,q) - M_{w'})^2}} \tag{4.4}$$

where M_w and $M_{w'}$ denote the mean intensity values of the original and extracted watermarks, respectively.

A series of simulated real-world attacks that could potentially damage the embedded watermark were employed to evaluate the robustness of the watermarked images. These attacks included filtering (average, Gaussian low-pass, and median), noise injection (Gaussian, speckle, and salt-and-pepper), geometric transformations (gamma correction and histogram equalization), and various image processing operations (JPEG compression, cropping, rotation, and scaling). The NC metric was then employed to quantify the resilience of the watermark after each attack.

4.3. **Experimental Results.** Table 1 shows NC values, which measure the similarity between the original watermark and the extracted watermark after various attacks were applied to five sample images. These values assess the robustness of our proposed watermarking scheme. The results are encouraging, with average NC values exceeding 0.9 for most attacks,

TABLE 1. NC values comparison on the host images

Attack	*F*16	*Baboon*	*Bridge*	*Peppers*	*Lena*	*Average*
$Salt-and-Pepper\ Noise(0.01)$	0.9616	0.9658	0.9647	0.9552	0.9543	0.96
$Gaussian\ Noise(0.01)$	0.8974	0.9421	0.9258	0.8775	0.8704	0.90
$Speckle\ Noise(0.01)$	0.9397	0.9643	0.9709	0.9637	0.9509	0.96
$Average\ Filtering(3\times 3)$	0.9403	0.7967	0.8880	0.9577	0.9580	0.90
$Gaussian\ low-pass(3\times 3)$	0.9803	0.9563	0.9695	0.9851	0.9844	0.98
$Gaussian\ low-pass(9\times 9)$	0.9801	0.9562	0.9694	0.9853	0.9842	0.98
$Median\ Filtering(3\times 3)$	0.9719	0.8651	0.9205	0.9761	0.9816	0.94
$Scaling(0.25)$	0.7947	0.6699	0.7284	0.8857	0.8738	0.79
$Rotate(45)$	0.8650	0.8435	0.9237	0.9018	0.9162	0.89
$Rotate(90)$	0.9744	0.9732	0.9762	0.9683	0.9806	0.97
$Gamma\ Correction(0.9)$	0.8629	0.8858	0.7854	0.8428	0.8695	0.85
$Crop(25\%)$	0.7370	0.5627	0.6404	0.8543	0.7767	0.71
$JPEG\ Compression(50)$	0.9879	0.9816	0.9865	0.9893	0.9889	0.98
Histogram Equalization	0.9760	0.9617	0.9819	0.9859	0.9844	0.98

TABLE 2. Transparency comparison on the host images

	*F*16	*Baboon*	*Bridge*	*Peppers*	*Lena*
$PSNR$	76.462	79.608	85.916	76.329	74.025
$SSIM$	1	1	1	1	1

signifying successful watermark retrieval. While the lowest average NC (0.71) occurs for a 25% cropping attack, the method exhibits its best performance against JPEG compression across all images.

The effectiveness of the proposed watermark embedding method in preserving image quality is evaluated in Table 2. PSNR and SSIM values, presented in the table, quantify the transparency of the watermarked images. Higher values indicate that the watermarks are well-hidden and do not significantly degrade the visual quality of the original images

4.4. **Comparitive Analysis.** Our method was evaluated against a related approach [6] using the Lena image. The PSNR value achieved by our method (74.025) surpasses that of the compared approach (32.12), signifying our method's superior ability to preserve image quality after watermark embedding.

Figure 2 further compares the robustness of both methods against various attacks. While the fuzzy c-mean method in [6] exhibits perfect robustness (NC=1) for Gaussian low-pass

filtering and slightly better performance for cropping at 25%, our method demonstrates overall competitive performance. Notably, our method outperforms the previous approach in terms of robustness against attacks like salt-and-pepper noise, median filtering, and JPEG compression, as shown by the consistently higher NC values.

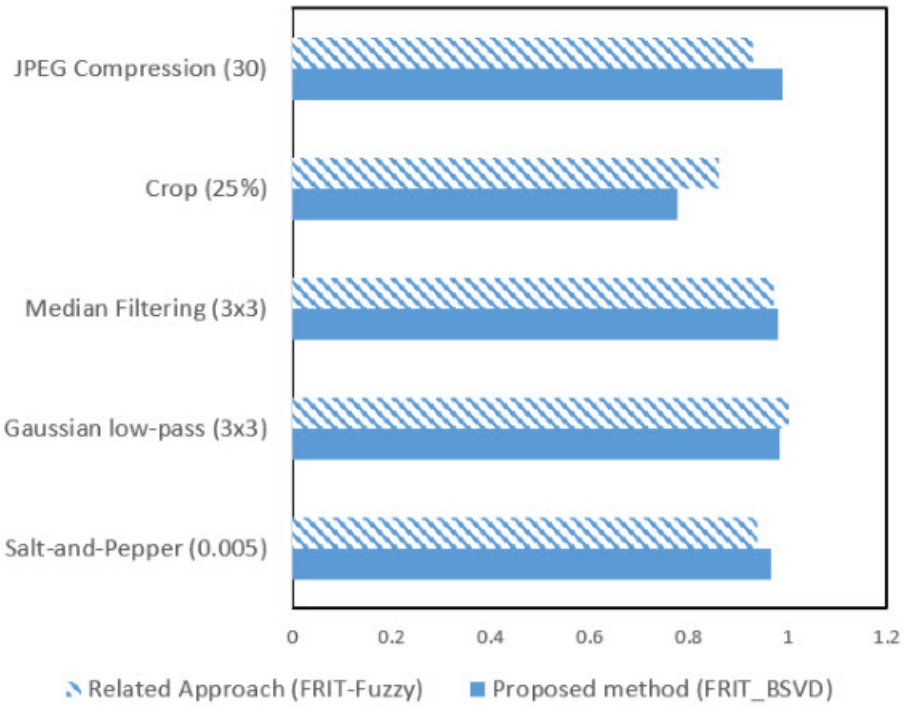

FIGURE 2. The comparison of the NC values between the proposed method and the approach FRIT-Fuzzy C-Mean [6] on Lena image.

Conclusion

This paper presented a watermarking method that uses the strengths of both FRIT and BSVD for robust and transparent watermark embedding. FRIT pre-processes the image to highlight key features, and BSVD decomposes it for targeted modification. The watermark information is then imperceptibly embedded by altering the singular values obtained from the FRIT coefficients. Our evaluation demonstrates the effectiveness of the proposed method. Watermarked images maintain high visual quality, as confirmed by PSNR and SSIM values in Table 1. Furthermore, Table 2 showcases the robustness of the method against various attacks, with high average NC values exceeding 0.9. Even in the case of a 25% cropping attack, the method exhibits acceptable robustness. Notably, it demonstrates superior resistance compared to a related approach, as shown by the NC values in Figure 2 for attacks like salt-and-pepper noise, median filtering, and JPEG compression.

Acknowledgments

The author would like to express their sincere thanks to Ms. Malihe Mardanpour for her valuable comments.

References

[1] A.k. Abdulrahman and S. Ozturk, A novel hybrid DCT and DWT based robust watermarking algorithm for color images. *Multimedia Tools and Applications*, **78**:17027–17049, 2019.

[2] G. Bhatnagar and B. Raman, Robust reference-watermarking scheme using waveletpacket transform and bidiagonal-singular value decomposition. *Int J ImageGraph* **9**(03):449–477, 2009.

[3] E. Candes and D.L. Donoho, Ridgelets: a key to higher dimensional intermittency. *Phil. Trans. R. Soc. Lond. A.* 2495–2509, 1999.

[4] M.N. Do and M. Vetterli, Orthonormal finite ridgelet transform for image compression. *IEEE Image Processing*, bf 2:367–370, 2000.

[5] J. Liu, J. Huang, Y. Luo, L. Cao, S. Yang, D. Wei and R. Zhou, An optimized image watermarking method based on HD and SVD in DWT domain. *IEEE Access*, **7**:80849–80860, 2019.

[6] H.Y.Y.J.L. Fan, A Blind Watermarking Using Orthogonal Finite Ridgelet Transform and Fuzzy C-Means. *Journal of Software*, **5**(4):429, 2010.

[7] M. Mardanpour and M.A.Z. Chahooki, Robust transparent image watermarking with Shearlet transform and bidiagonal singular value decomposition. *AEU-International Journal of Electronics and Communications*, **70**(6):790–798, 2016.

[8] P. Mitra, R. Gunjan and M. S. Gaur, *A multi-resolution watermarking based on contourlet transform using SVD and QR decomposition*, *International Conference on Recent Advances in Computing and Software Systems (RACSS)*, 135–140, 2012.

[9] M. Moosazadeh and G. Ekbatanifard, A new DCT-based robust image watermarking method using teaching-learning-based optimization. *Journal of Information Security and Applications*, **47**:28–38, 2019.

[10] P. Parashar and R.K. Singh, A survey: digital image watermarking techniques. *International Journal of signal processing, image processing and pattern recognition*, **7**(6):111–124, 2014.

[11] P. Premaratne, C.C. Ko, *A novel watermark embedding and detection scheme for images in DFT domain*, *Inter. Conf. on Image Processing and Its Applications*, 780, 1999.

[12] S. Rawat and B. Raman, Best tree wavelet packet transform based copyright protection scheme for digital images. *Optics Communications*, **285**(10-11):2563–2574, 2012.

[13] D. Singh and S.K. Singh, DWT-SVD and DCT based robust and blind watermarking scheme for copyright protection. *Multimedia Tools and Applications*, **76**(11):13001–13024, 2017.

[14] S. Sharma, J.J. Zou, G. Fang, P. Shukla and W. Cai, A review of image watermarking for identity protection and verification. *Multimedia Tools and Applications*, **83**(11):31829–31891, 2024.

[15] L. Zhang and D. Wei, Dual DCT-DWT-SVD digital watermarking algorithm based on particle swarm optimization. Multimedia Tools and Applications, **78**:28003–28023, 2019.

(Farzaneh Salari) Department of Mathematics, , Faculty of Sciences, Razi University, Kermanshah, Iran.

Email address: f.salari@razi.ac.ir